Mechanical Behaviour of Soil under Drying-wetting Cycles and Vertical Confining Pressure

Author 1

Zhiming Chao[#], Associate Professor

Shanghai Maritime University, Shanghai, China

Failure Mechanics and Engineering Disaster Prevention, Key Laboratory of Sichuan Province, Sichuan University, Chengdu, China, 610065

School of Engineering, University of Warwick, CV4 7AL, UK

Author 2

Danda Shi[#], Professor

Shanghai Maritime University, Shanghai, China

Author 3

Gary Fowmes*, Reader

School of Engineering, University of Warwick, CV4 7AL, UK

***Corresponding author**

[#]The authors contribute equally

E-mail: zmchao@shmtu.edu.cn

Abstract

A system for preparing soil specimens subjected to drying-wetting cycles whilst under vertical confining pressures is introduced with Clayey soil specimens subjected to different drying-wetting histories, then the relative performance tested using consolidated undrained triaxial shear tests. Meanwhile, their soil water retention properties were also measured. The experimental results indicate that drying-wetting cycles lead to a rise in the matric suction for soil with high moisture content, and the decrease of matric suction for soil with low moisture content. Partly owing to the higher pore water pressure, peak shear strength reduces gradually during drying-wetting cycles. The impacts of drying-wetting cycles on hydro-mechanical properties of soil specimens during the first cycle are larger than those during the second and the third cycles as the highest matric suction of soil occurs during the first cycle. Vertical confining pressure is shown to limit the impact of drying-wetting cycles on the hydro-mechanical properties of soil effectively because of its restricting effects on the volumetric deformation of soil during the cycles.

Keywords: Clays; Expansive soils; Pore structure; Shear strength

1 Introduction

Near surface soil is inevitably subject to climatic effects and will experience periodical drying-wetting cycles. Drying-wetting cycles can alter the hydro-mechanical characteristics (Mechanical properties and pore water pressure) of soil, and affect the performance of the soil in various engineering applications (Chao and Fowmes, 2022; Tang et al., 2016). For example, clayey soils are often adopted as the cover soil of landfills to prevent the contamination of waste to the surrounding environment. During the operational phase of the landfills, drying-wetting cycles may reduce the mechanical strength of the cover soil, leading to the instability of cover system (Chao et al., 2023b; Wang et al., 2022), especially under extreme climatic conditions such as long-term alternating heavy rainfall and drought. Multiple drying-wetting cycles may induce engineering problems including the failure of engineering facilities caused by the weakening hydro-mechanical properties of soil (Shao et al., 2023; Wang et al., 2016; Xu et al., 2022; Zhang et al., 2023a; Zhang et al., 2023b). Thus, knowledge of the soil response to climate loading, in particular to drying-wetting cycles, is vital for the application of soil in engineering infrastructures.

In practical engineering, most of soil also bears in situ vertical confining pressure that is generated by overlaying soil, buildings, etc (Chao et al., 2022a; Chao et al., 2022b; Chao et al., 2023a; Cui et al., 2022a; Cui et al., 2022b; Liu, 2015; Miao et al., 2019;). Many scholars have pointed out that during drying-wetting cycles, volume change of soil are the main reason for variation in the hydro-mechanical characteristics of soil, especially for clayey soil (Cui et al., 2018; Cui et al.,2022; Cui et al., 2023; Cuisinier et al., 2014; Li et al., 2022; Shu et al., 2022;). Meanwhile, researchers have validated that the vertical confining pressure can effectively restrict the volumetric deformation of soil during drying-wetting cycles (Estabragh et al., 2015; Tang et al., 2019; Gastelo et al., 2023). Thus, the vertical confining pressure is an essential influence factor that needs to be considered when evaluating the hydro-mechanical behaviour of soil subjected to drying-wetting cycles.

In recent years, a number of experimental investigations have been carried out to consider the impacts of drying-wetting cycles on the hydro-mechanical properties of soil under different stress statuses (Cui et al., 2021; Meng et al., 2020; Rosone et al., 2018; Stoltz et al., 2014;). Aldaood et al. (2014) prepared soil specimens subjected to moisture content-controlled cycles by immersing soils in water then drying them at a temperature of 60 ℃, and unconfined compression tests were conducted on the soil specimens. Li et al. (2018) carried out direct shear tests and unconfined compressive tests on Loess subjected to cyclically adding water from a burette and drying in air. Zhang et al. (2018) performed direct shear tests on Silt subjected to cyclic submerging in water and drying in air. The existing research all indicates that drying-wetting cycles have negligible detrimental impacts on the mechanical properties of soil (Li et al., 2021). For expansive clayey soil, drying-wetting cycles can result in expansion and shrinkage which can cause the generation of internal cracks, significantly reducing the strength of clayey soil (Zainab et al., 2021). The Mercia Mudstone Clay used in this investigation has been rarely reported in the literature and is extensively applied in engineering structures as building material, such as the landfills in the UK. Thus, it pressingly needs to analyse the hydromechanical properties of Mercia Mudstone Clay under combined effects of vertical confining pressure and drying-wetting cycles as well as compare with that of Kaolin Clay.

In this paper, based on the preparation system of soil specimens subjected to drying-wetting cycles under different vertical confining pressures, the corresponding Mercia Mudstone Clay and Kaolin Clay samples were prepared and a series of consolidated undrained triaxial compression tests were carried out on the prepared soil specimens subjected to drying-wetting cycles under different vertical confining pressure; Meanwhile, the soil water characteristic curves (SWCCs) of soil specimens during different drying-wetting cycles were measured. The obtained experimental results allow the hydro-mechanical response of Mercia Mudstone Clay and Kaolin Clay under different vertical confining pressures subjected to drying-wetting cycles to be analysed, and the corresponding affecting mechanism is revealed.

2 Clayey Soil Materials

Two types of clayey soils were adopted in this paper: (1) Kaolin Clay and (2) Mercia Mudstone Clay, both derived from the UK. The reason for selecting the two types of soil is to investigate and compare the influence of drying-wetting cycles on the hydro-mechanical characteristics of clayey soils with different plasticity. The basic parameters for the two types of clayey soils are presented in Table 1. In Table 1, the maximum dry density refers to the highest dry density of soil under a certain moisture content, and the optimum moisture content refers to the moisture content that soil can reach the maximum dry density.

Table 1. The basic parameters of clayey soil specimens

Properties	Kaolin Clay	Mercia Mudstone Clay
Liquid limit (%)	47.0	33.6
Plastic limit (%)	26.6	17.4
Plasticity index (%)	20.4	16.2
Maximum dry density (g/cm^3)	2.00	1.93
Optimum moisture content (%)	20.0	11.8
Saturated moisture content (%)	56.36	68.43
Soil particle passing 2 mm (%)	100	100
Soil particle passing 1 mm (%)	100	100
Soil particle passing 0.1 mm (%)	100	100
Soil particle passing 0.05 mm (%)	92	74

3 Experimental Programme

3.1 Triaxial Soil Specimen Preparation

The soil specimens experienced drying-wetting cycles under vertical confining pressure inside a 3D printed PLA (Poly Lactic Acid) mould, with load being applied by dead weights that were placed on the cap of the mould to impose vertical loading. In the preparation process, soil specimens for triaxial tests were housed inside the assembled 3D printed mould. During the wetting process, the set of moulds containing soil specimens were placed in a water tank and immersed in water for 24 h, and during the drying process, they were housed in a sealed box to dry by utilising a heating system for 24 h under the constant temperature of 40 ℃. The heating system consists of a sealed box, two ceramic heating lamps with thermostats, and two temperature sensors, creating a closed loop feedback system. It is shown in Figure 1. The Kaolin Clay and Mercia Mudstone Clay specimens, subjected to either 0, 1 and 3 drying-wetting cycles, were prepared with vertical confining pressures of 0 kPa, 25 kPa and 50 kPa.

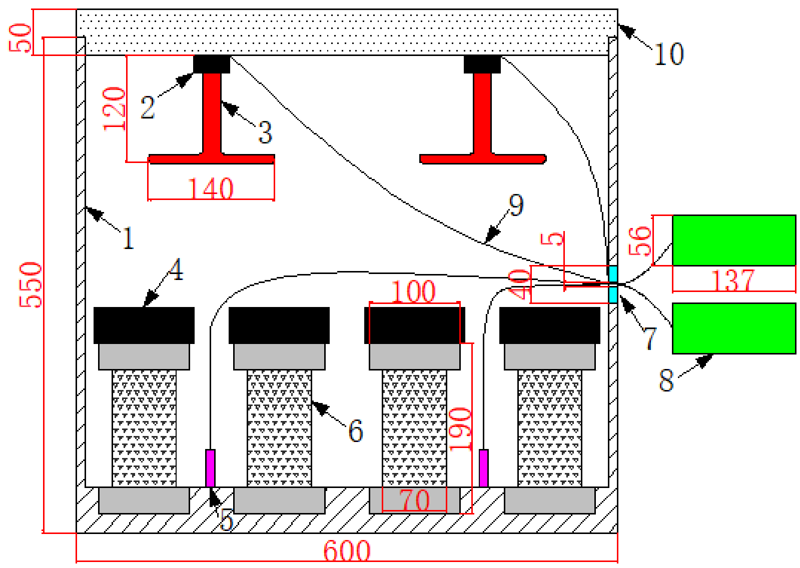

1. Wooden sealed box 2. Ceramic lamp cap 3. Ceramic heating lamp 4. Dead weights 5. NTC temperature sensor 6. 3D printed mould and soil specimens 7. Hole and cylindrical lid 8. Microcomputer thermostat 9. Power line for the ceramic heating lamp 10. Lid for the box

Figure 1. The schematic diagram of the heating system

3.2 The Measurement of SWCC

SWCC represents the relationship between matric suction of unsaturated soil and moisture content, which is a basic property curve for unsaturated soil, characterizing the water holding capacity of unsaturated soil with different matric suctions. In this paper, the filter paper method was employed to measure the drying curves of SWCC for soil specimens subjected to 0, 1, and 3 numbers drying-wetting cycles under 0 kPa vertical confining pressure based on ASTM-D5298 (AC07566974, 2003). The filter paper method is a common approach to measure the SWCC of soil, which is reliable.

3.3 Triaxial Shear Test

The consolidated undrained triaxial shear tests were conducted on the prepared soil specimens using the conventional Triaxial System following ASTM D7181 (ASTM, 2011). In this experiment, the effective cell pressure was set as 20 kPa, 35 kPa and 50 kPa, respectively, and the soil specimen was sheared at a strain rate of 0.1 % min. The shearing was terminated when the shear strain reached 15 %. The triaxial shear test is a general method to measure the mechanical properties of soil, which is reliable. The detailed experimental scheme is listed in Table 2. All the experimental operation in this manuscript is according to the requirement of British Standard and ASTM.

Table 2. The experimental scheme

Soil type	Drying-wetting cycle	Vertical confining pressure (kPa)	Cell pressure (kPa)
Kaolin Clay, Mercia Mudstone Clay	0	0	20,35,50
	1	0,25,50	
	3		

4 Experimental Results

4.1 SWCC of Soil

Figure 2 presents the SWCCs of Kaolin Clay and Mercia Mudstone Clay specimens subjected to 0, 1 and 3 numbers drying-wetting cycles under 0 kPa vertical confining pressure.

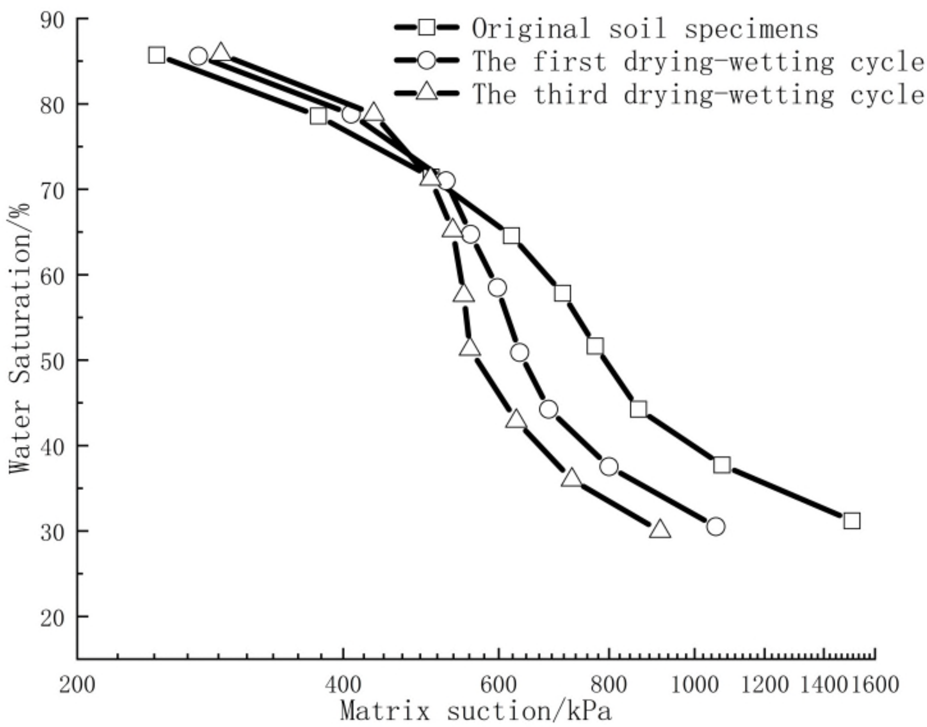

(a) Kaolin Clay

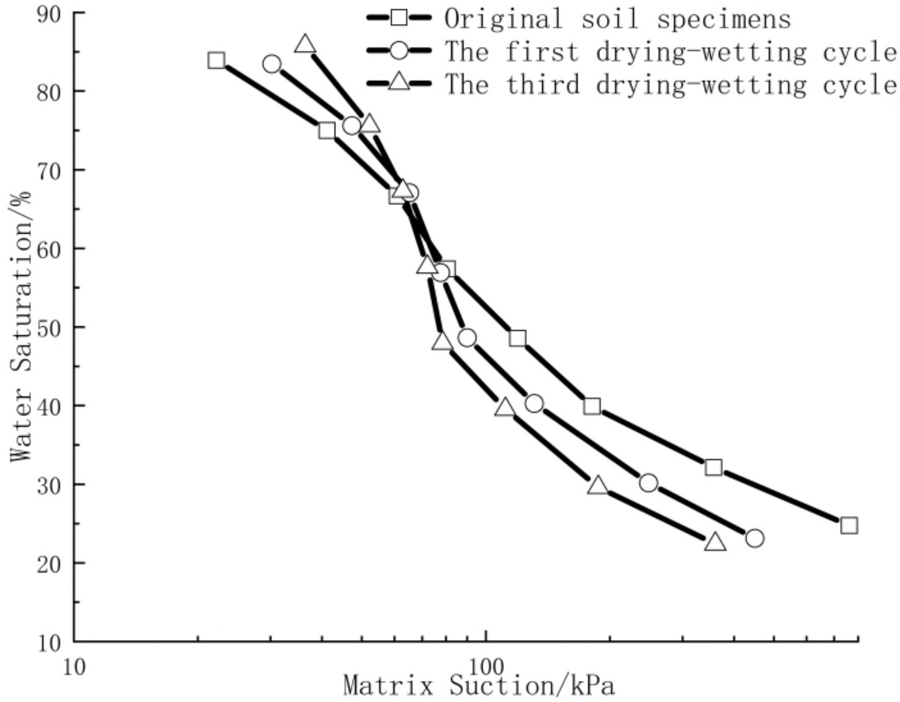

(b) Mercia Mudstone Clay

Figure 2. The SWCCs of soil specimens

Based on Figure 2, at high moisture saturation, the matric suction of soil specimens with high number of drying-wetting cycles is larger than that with low number of cycles. In contrast, at low moisture content, the opposite trend is observed. The turning point for Kaolin Clay is about 70.20 % moisture saturation with 500 kPa matric suction, and for Mercia Mudstone Clay, it is around 60.26 % moisture saturation with 60 kPa matric suction. Additionally, it should be noted that the impacts of drying-wetting cycles on the SWRCs of Mercia Mudstone Clay are larger than those for Kaolin Clay. Moreover, for both of Kaolin Clay and Mercia Mudstone Clay specimens, the first drying-wetting cycle has significantly larger impacts on the SWRCs than the second and the third cycles. For example, at 42.86 % moisture saturation, the matric suction decreases by 20.94 % and 24.37 % during the first cycle for Kaolin Clay and Mercia Mudstone Clay, respectively, whereas, during the second and the third cycles, the matric suction falls by 8.05 % and 12.22 %, respectively. It also can be seen that, at the same moisture saturation, the matric suction for Kaolin Clay specimen is higher than that of Mercia Mudstone Clay specimens, which means that at the same matric suction, the moisture saturation for Kaolin Clay is higher and it has stronger water retention capacity. For example, for the original soil sample, at the moisture saturation of 60 %, the matric suction of Kaolin Clay is 560 kPa, while the value for Mercia Mudstone Clay is 79 kPa. This can be attributed to the portion of fines content for Kaolin Clay is higher than that of Mercia Mudstone Clay, as shown in Table 1, which indicates that the average pores size of Kaolin Clay is smaller than that of Mercia Mudstone Clay and the capillary action in Kaolin Clay is stronger (Haghighi, 2011).

4.2 Shear Deformation of Kaolin Clay in Triaxial Tests

Deviatoric stress versus axial strain curves for Kaolin Clay specimens are shown in Figure 3.

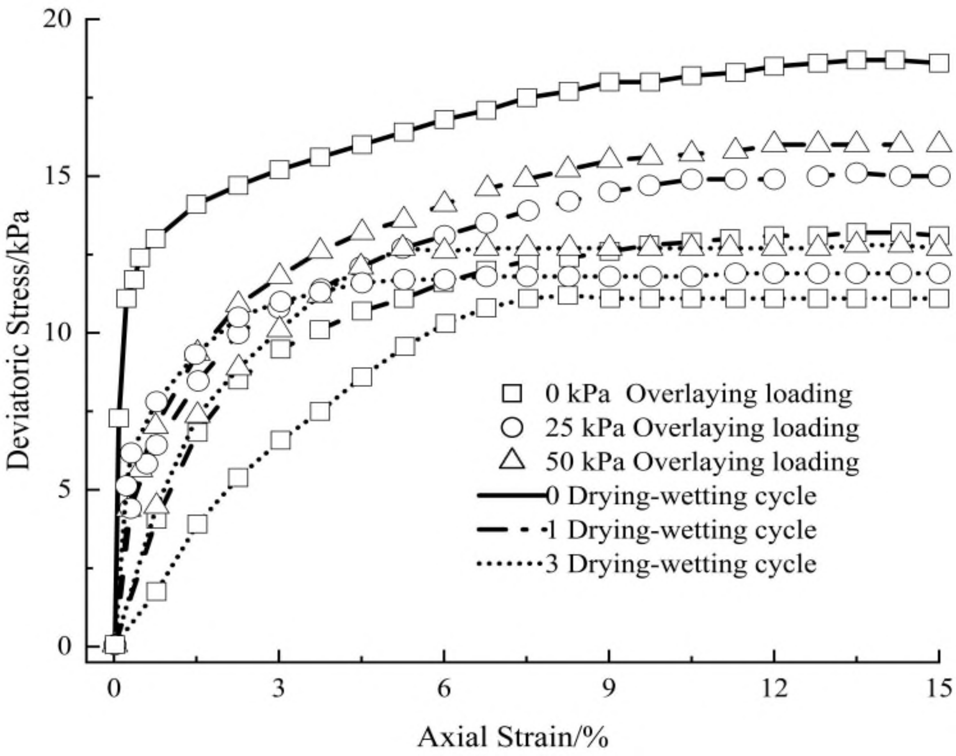

(a) 20 (kPa) Cell pressure

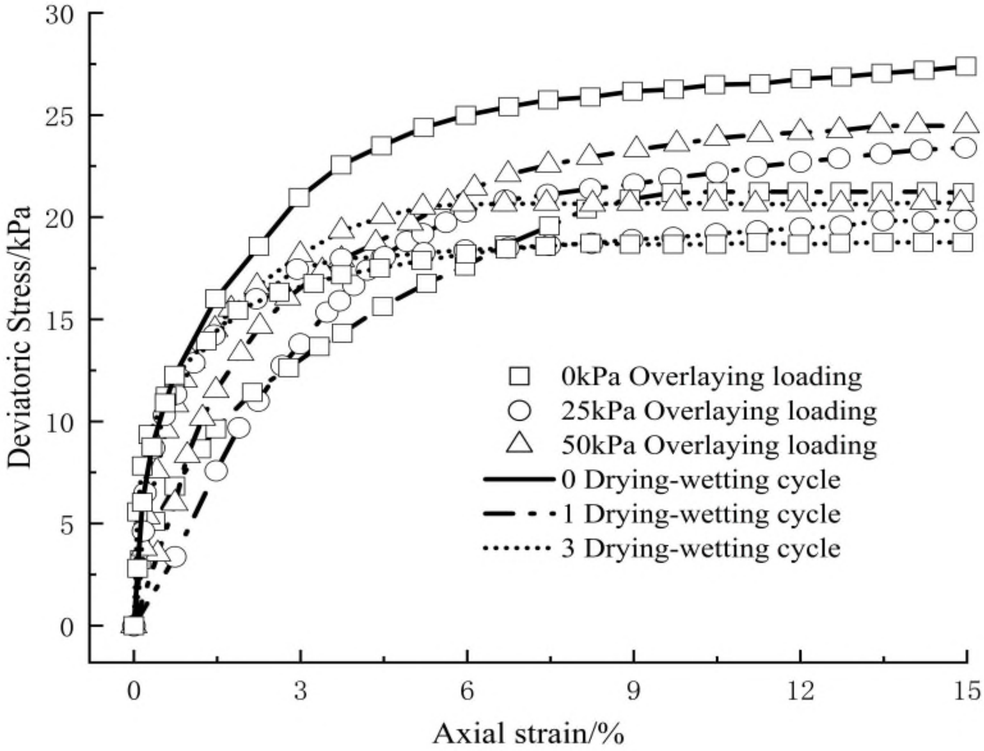

(b) 35 (kPa) Cell pressure

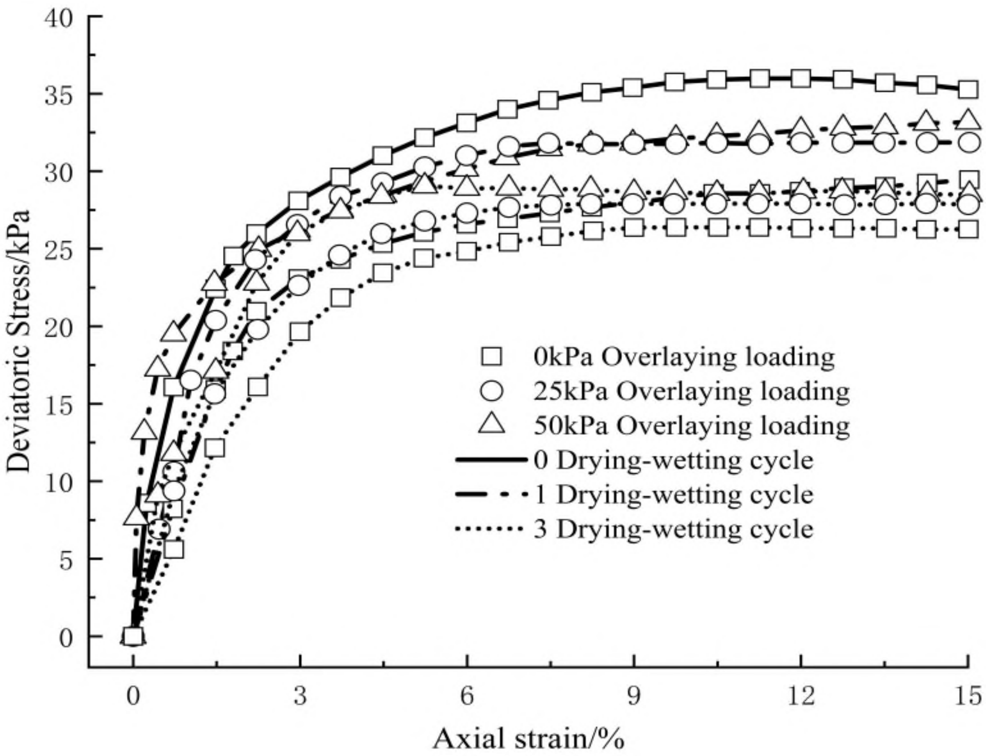

(c) 50 (kPa) Cell Pressure

Figure 3. The relationship curves between deviatoric stress and axial strain for Kaolin Clay

Based on Figure 3, the deviatoric stress-axial strain relationship of Kaolin Clay specimens appears to be strain-hardening. The results also show that the peak shear strength reduces gradually with the rise in the number of drying-wetting cycles. More specifically, the reduction is more pronounced in the first cycle than that in the second and third cycle, respectively. Taking the Kaolin Clay specimen under 0 kPa vertical confining pressure in 35 kPa cell pressure as an example, after the first cycle, the peak shear strength decreases by 23.67 %, while after the second and third cycles, it reduces by 7.67 %. Additionally, for the same number of drying-wetting cycles, the peak shear strength of Kaolin Clay specimen under high vertical confining pressure is larger than that under low vertical confining pressure. For example, under 50 kPa cell pressure, for the specimen under 0 kPa vertical confining pressure, the peak shear strength reduces by 12.98 % during the first cycle and 9.8 % during the second and third cycles. In comparison, for the specimen under 25 kPa vertical confining pressure, the peak shear strength decreases by 12.49 % and 8.92 %, respectively. Moreover, the impacts of cell pressure on the peak shear strength of soil specimen subjected to drying-wetting cycles are larger than the original specimen. For instance, from cell pressure 20 kPa to 50 kPa, the peak shear strength of original Kaolin Clay specimen, increases by about 1.8 time, while for the specimen under 0 vertical confining pressure during 3 numbers of drying-wetting cycles, the peak shear strength rises by around 2.5 times.

4.3 Shear Deformation of Mercia Mudstone Clay in Triaxial Tests

Deviatoric stress versus axial strain curves for Mercia Mudstone Clay specimens are shown in Figure 4.

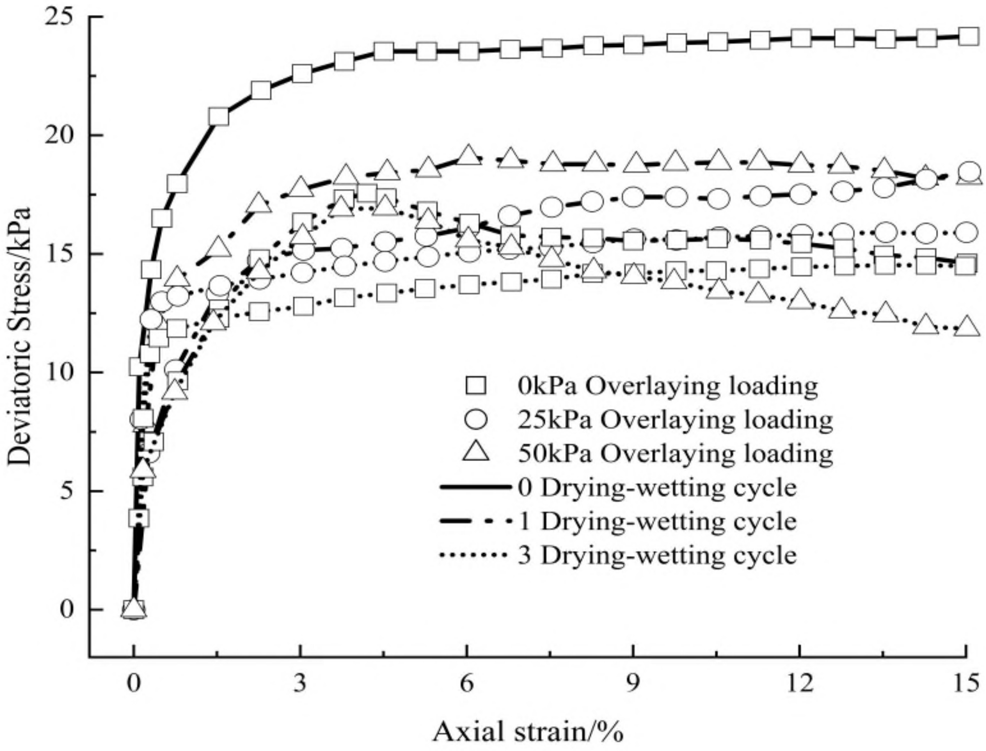

(a) 20 (kPa) Cell pressure

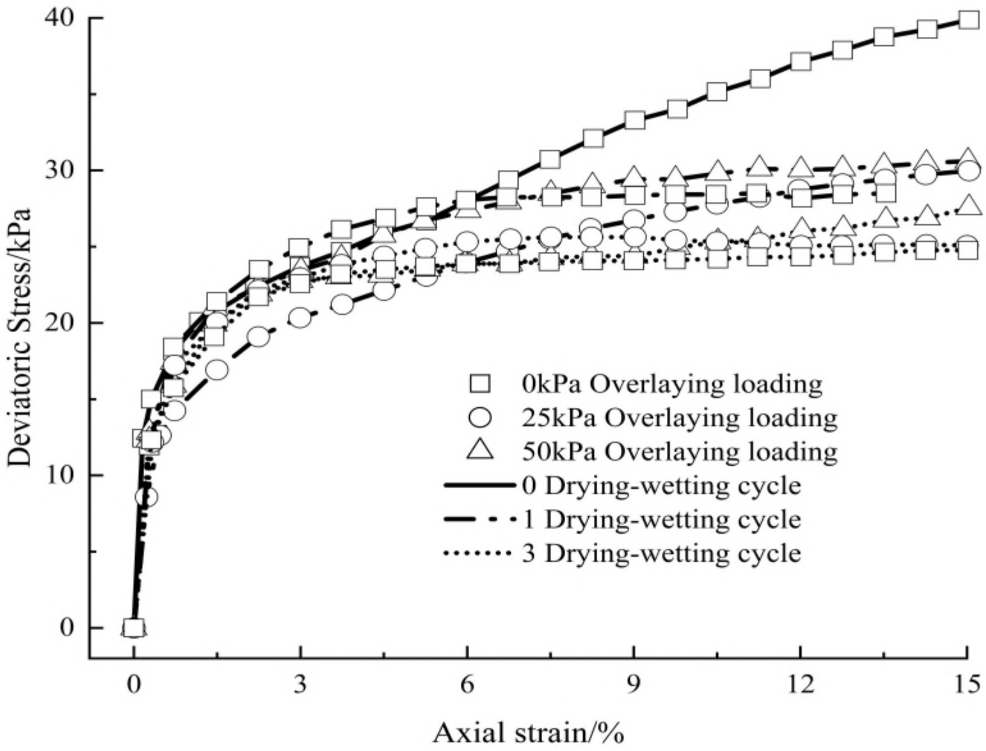

(b) 35 (kPa) Cell pressure

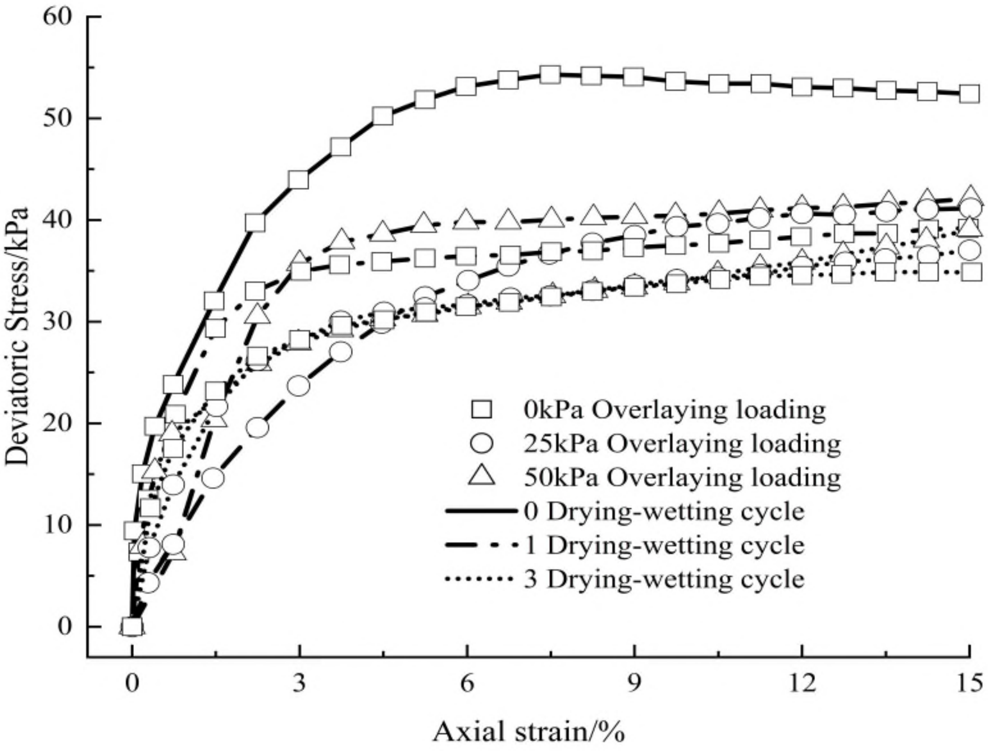

(c) 50 (kPa) Cell pressure

Figure 4. The relationship curves between deviatoric stress and axial strain for Mercia Mudstone Clay

As seen in Figure 4, the deviatoric stress versus axial strain curves of Mercia Mudstone Clay specimens are also typically of the strain-hardening type, but the peak shear strength of Mercia Mudstone Clay is larger than that of Kaolin Clay. The peak shear strength of Mercia Mudstone Clay reduces gradually with the rise of drying-wetting cycle as well, and the reduction is more pronounced in the first cycle than that in the second and third cycles. However, the magnitude of peak shear strength for Mercia Mudstone Clay is significantly higher than that of Kaolin Clay. Taking the soil specimens under 0 kPa vertical confining pressure in 50 kPa cell pressure as an example, after the first drying-wetting cycle, for Mercia Mudstone Clay, the peak shear strength decreases by 24.94 %, while after the third cycle, it reduces by 32.60 %. In comparison, for Kaolin Clay, the peak shear strength decreases by 12.96 %, while after the third cycle, it reduces by 22.76 %. Furthermore, as with Kaolin Clay, for the same number of drying-wetting cycles, the peak shear strength of Mercia Clay specimen under high vertical confining pressure is larger than that under low vertical confining pressure. For example, for the Mercia Mudstone Clay subjected to one drying-wetting cycle under 20 kPa cell pressure, the peak shear strength of sample under 0 kPa vertical confining pressure is 17 kPa, while the value is 19 kPa under 50 kPa vertical confining pressure. In terms of the influences of cell pressure, the Mercia Mudstone Clay specimens subjected to drying-wetting cycles are also more sensitive to cell pressure loading than that of original specimens. For example, when cell pressure is loaded from 20 kPa to 50 kPa, the peak shear strength of original Mercia Mudstone Clay sample under 0 vertical confining pressure rises 31 kPa, while the increasing magnitude of Mercia Mudstone Clay sample subjected to 3 drying-wetting cycles is 20 kPa.

4.4 The Pore Water Pressure of Kaolin Clay

The pore water pressure versus axial strain curves for Kaolin Clay specimens are shown in Figure 5.

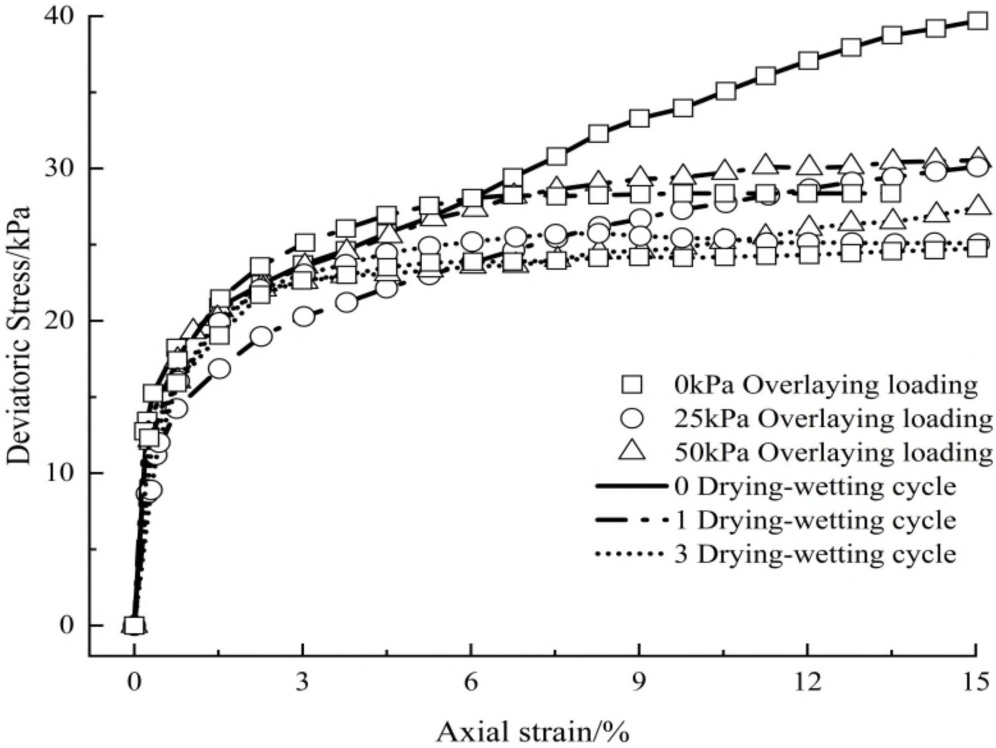

(a) 20 (kPa) Cell pressure

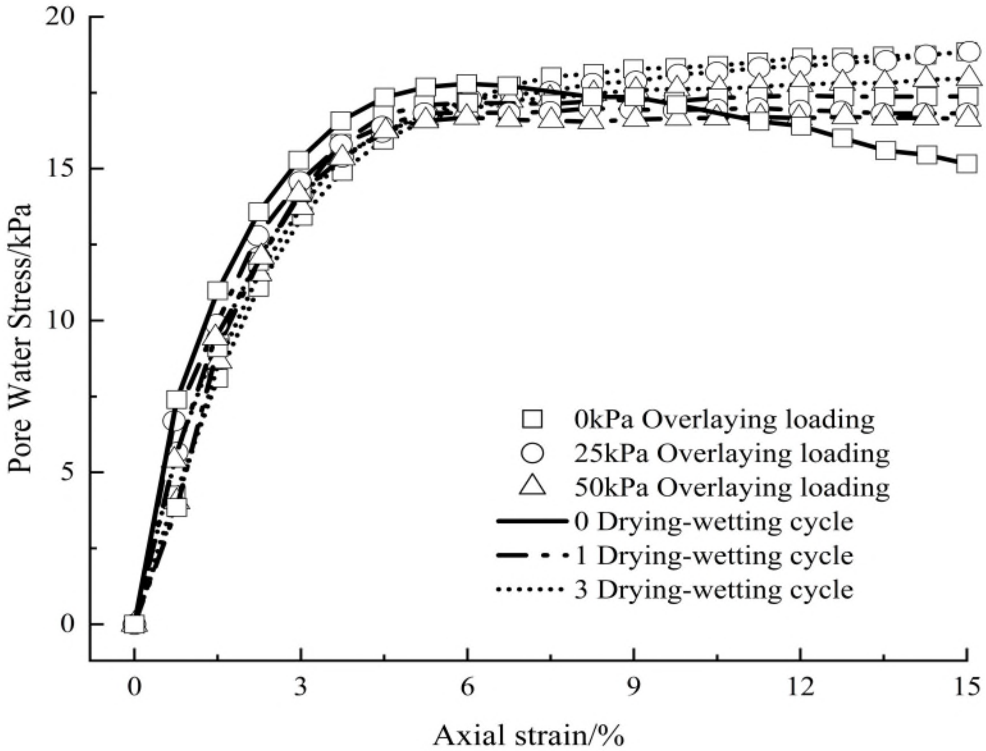

(b) 35(kPa) Cell pressure

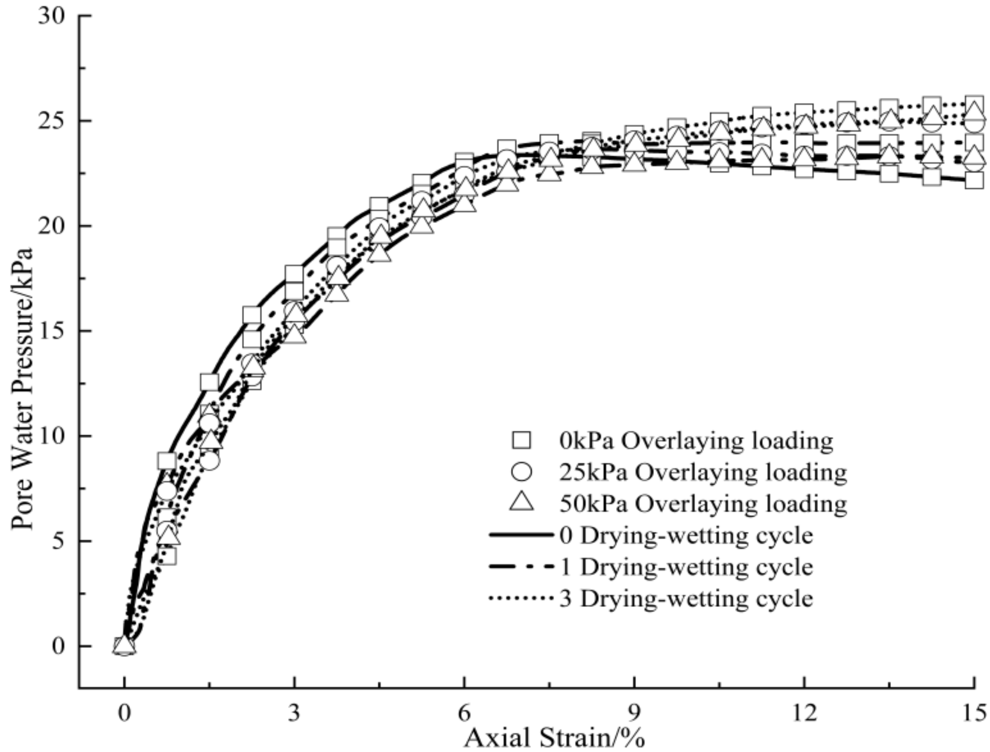

(c) 50(kPa) Cell pressure

Figure 5. The relationship curves between pore water pressure and axial strain for Kaolin Clay

Based on Figure 5, for original Kaolin Clay specimens, with the rise of axial strain, the pore water pressure increases gradually, after reaching the maximum pressure level, there is a slight reduction. In comparison, for Kaolin Clay specimens subjected to drying-wetting cycles, the pore water pressure tends to reach a steady state or increases continuously with the rising axial strain. More specifically, in the initial shearing stage, the pore water pressure of specimens subjected to drying-wetting cycles is lower than that of the original specimen, while with further shearing, the pore pressure of specimens subjected to drying-wetting cycles overtakes that of original specimens. At the end of the tests, the pore water pressure curves of specimens subjected to multiple cycles of drying-wetting are above that of the original specimen and the specimen subjected to one cycle. Additionally, the variation rules of pore water pressure for Kaolin Clay samples under different vertical confining pressure are similar.

4.5 The Pore Water Pressure of Mercia Mudstone Clay

The pore water pressure versus axial strain curves for Mercia Mudstone Clay specimens are shown in Figure 6.

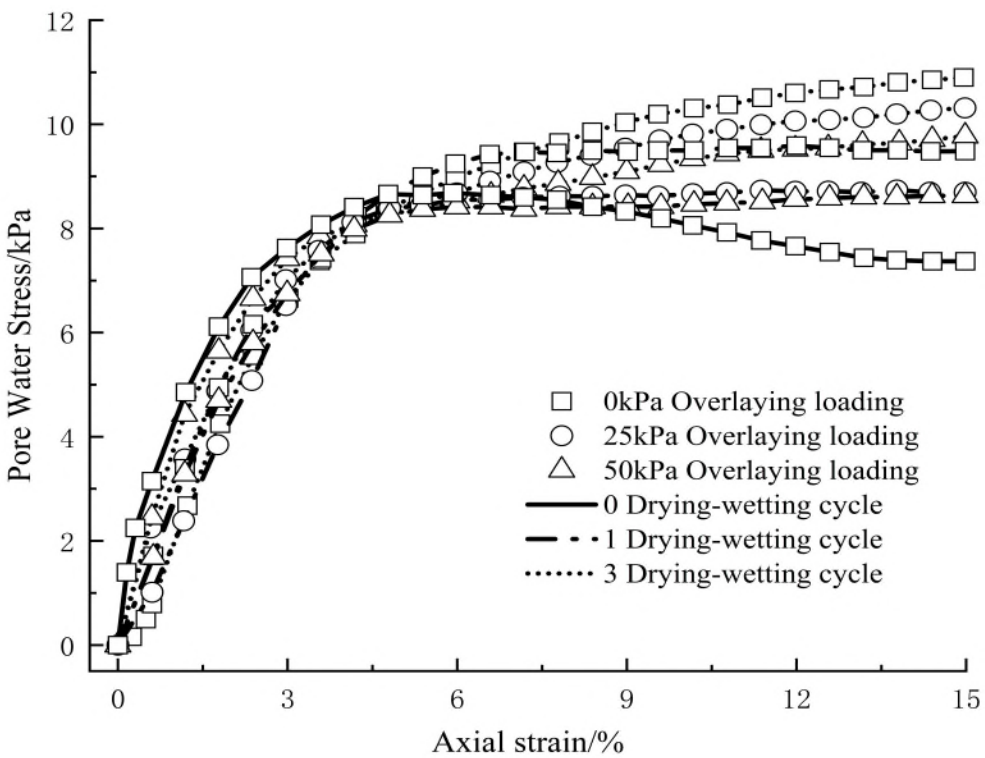

(a) 20 (kPa) Cell pressure

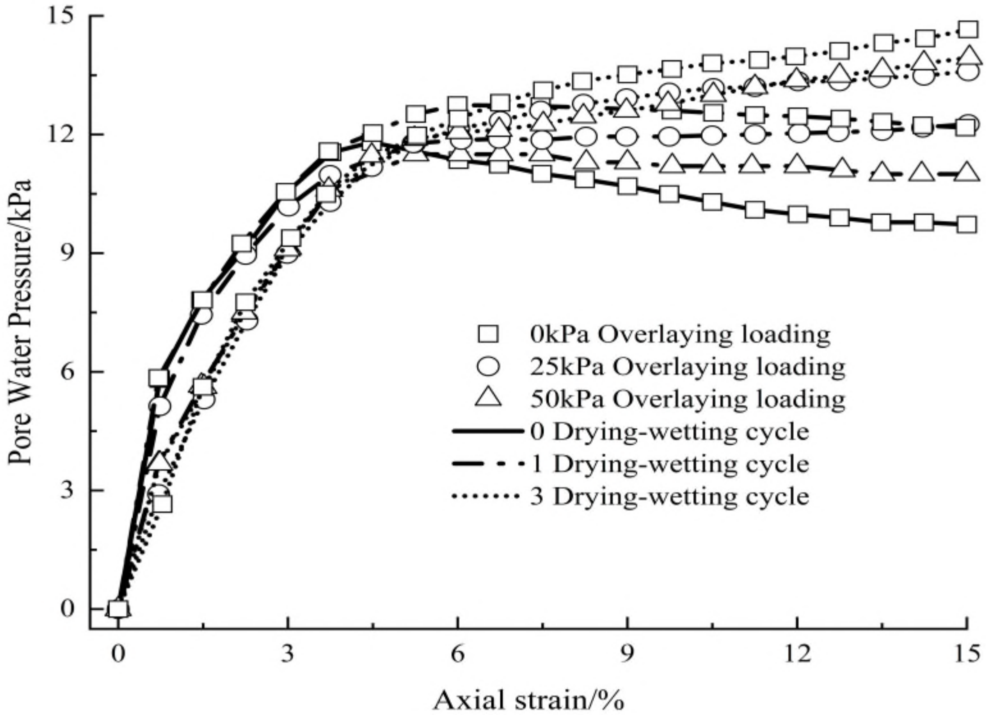

(b) 35 (kPa) Cell pressure

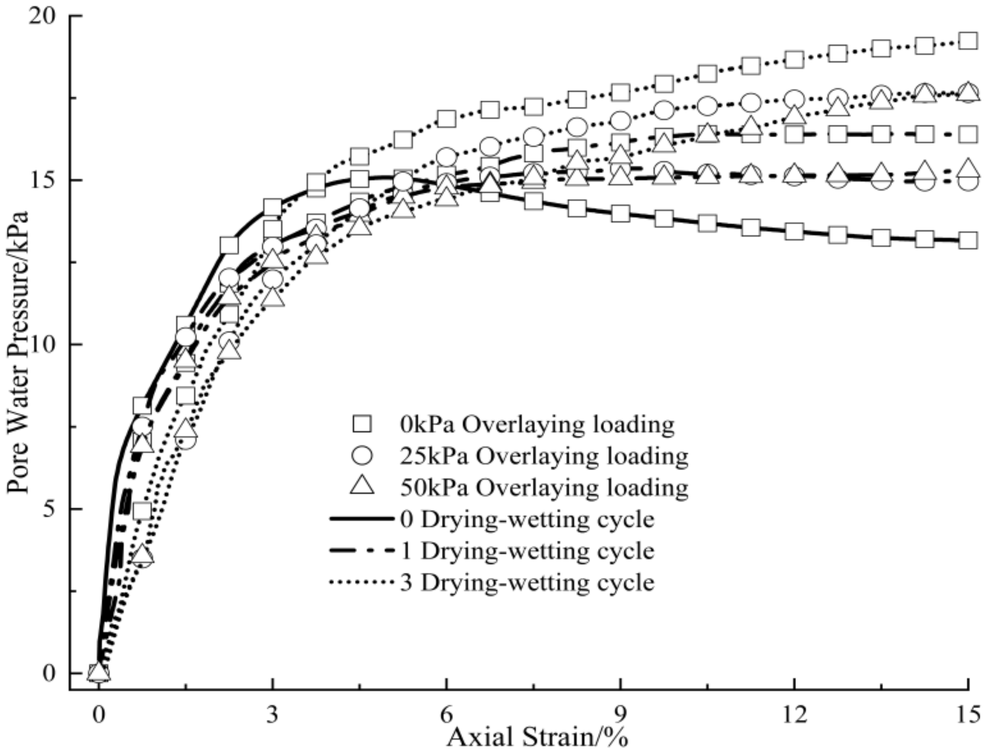

(c) 50 (kPa) Cell pressure

Figure 6. The relationship curves between pore water pressure and axial strain for Mercia Mudstone Clay

Based on Figure 6, the pore water pressure of Mercia Mudstone Clay is less than that of Kaolin Clay. Also, the same as Kaolin Clay specimens, the pore water pressure of original Mercia Mudstone Clay specimens subjected to drying-wetting cycles is larger than that of original soil specimens. For example, under 50 kPa cell pressure, the peak pore water pressure of Mercia Mudstone Clay sample subjected to three drying-wetting cycles under 0 kPa vertical confining pressure is 19 kPa, while the value of the original sample is 15 kPa. Moreover, as in Kaolin Clay specimens, the influence of the first cycle on pore water pressure for Mercia Mudstone Clay specimens is larger than that of the second and the third cycles. However, in general, the impacts of drying-wetting cycles on pore water pressure of Mercia Mudstone Clay specimens are larger than that of Kaolin Clay specimens. Additionally, as with that of Kaolin Clay, the variation rules of pore water pressure for Mercia Mudstone Clay samples under different vertical confining pressure are similar.

4.6 The Effective Stress Paths of Soil Specimens

Based on the experimental results, the effective stress paths of Kaolin Clay and Mercia Mudstone Clay specimens are drawn in Figure 7 and Figure 8, respectively. On each effective stress path, one failure point is indicated, as shown in Figure 7 and Figure 8. The meaning of failure point here is the point with the maximum of stress ratio (effective deviatoric stress divided by effective mean stress) on effective stress paths.

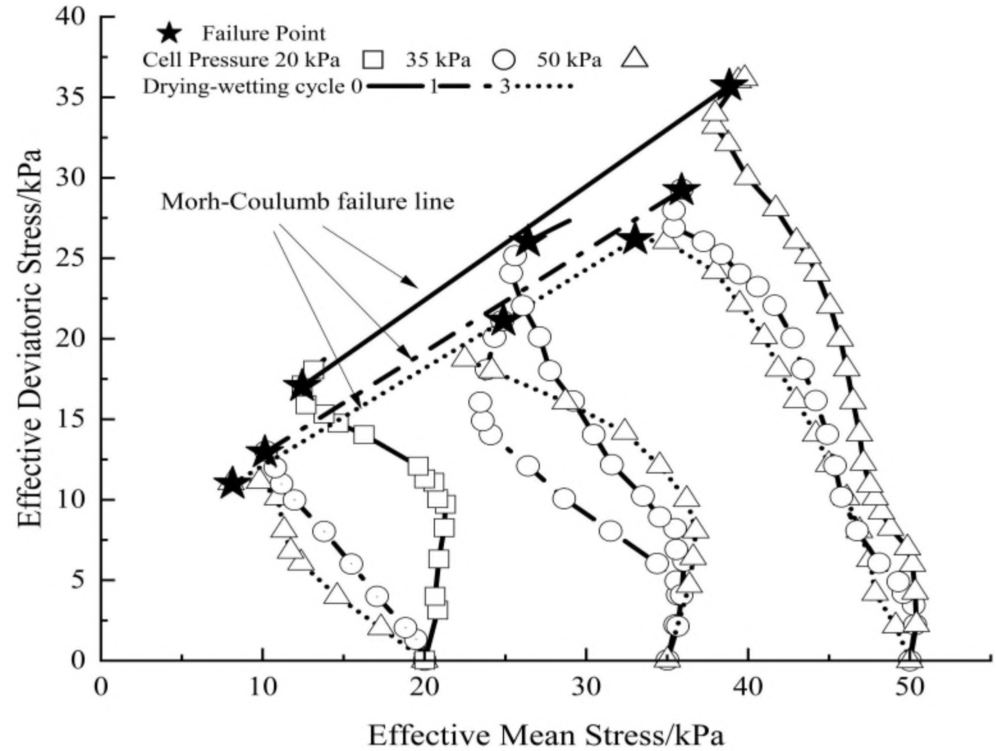

(a) 0 (kPa) Vertical confining pressure

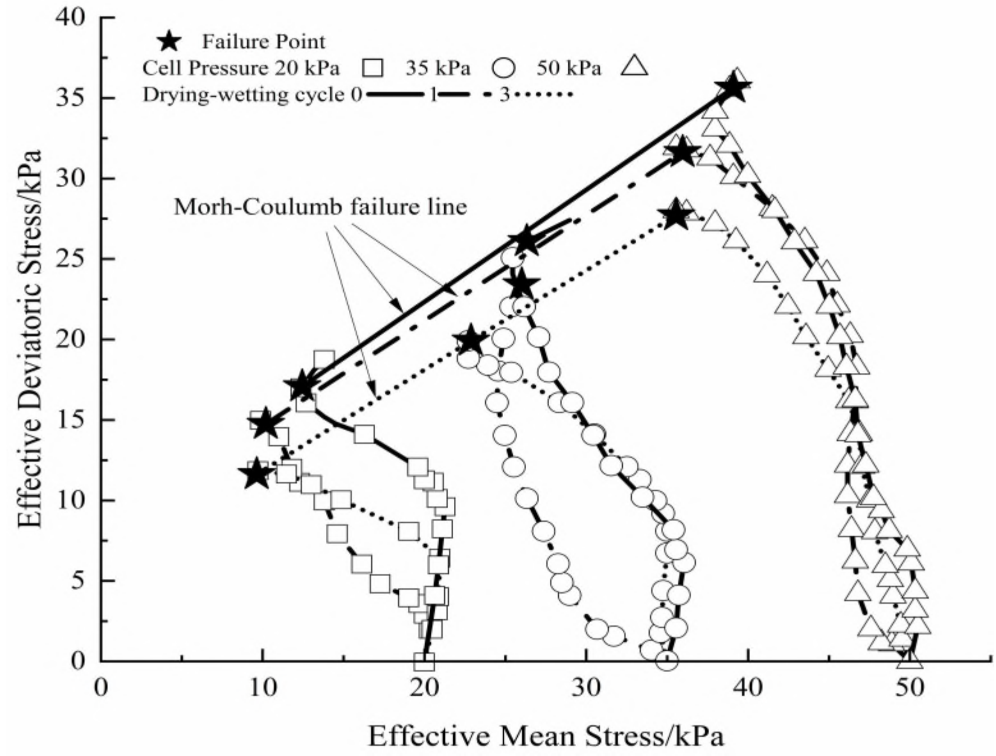

(b) 25 (kPa) Vertical confining pressure

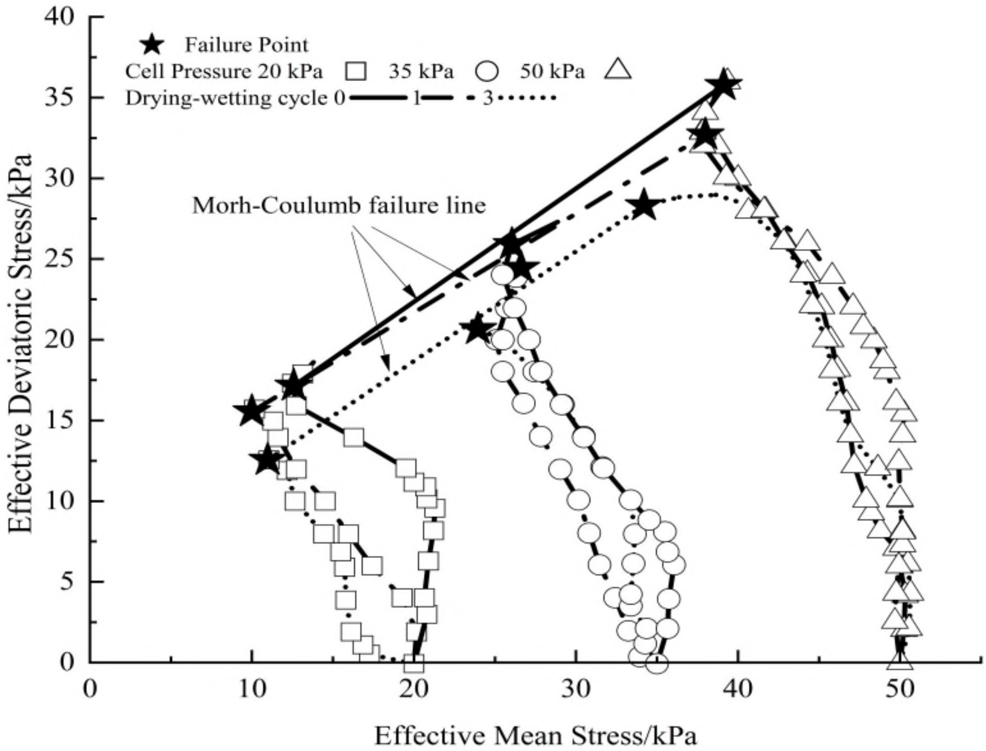

(c) 50 (kPa) Vertical confining pressure

Figure 7. The effective stress paths of Kaolin Clay

Based on Figure 7, the effective stress paths for the original Kaolin Clay specimens and Kaolin Clay specimens subjected to drying-wetting cycles are different. For original specimens, the shape of effective stress paths is similar to the “S” shaped curve. In comparison, for Kaolin Clay specimens subjected to drying-wetting cycle, with the rise of effective deviatoric stress, most of stress paths traverse to the left from their initial isotropic state due to the rapid rise of pore water pressure. Then, the effective mean stress continues to reduce with the increase of effective deviatoric stress until reaching the failure point. Additionally, in general, the stress paths of soil specimens subjected to drying-wetting cycle are located to the left of the stress paths of original soil specimens due to the larger pore water pressure of soil specimens subjected to the cycles. Moreover, it is also worth noting that, for soil specimens subjected to a higher number of drying-wetting cycles, their failure points are located at a lower effective deviatoric stress and effective mean stress. Additionally, under the same confining pressure, the effective deviatoric stress of failure points for Kaolin Clay samples under high vertical confining pressure is larger than that under low vertical confining pressure.

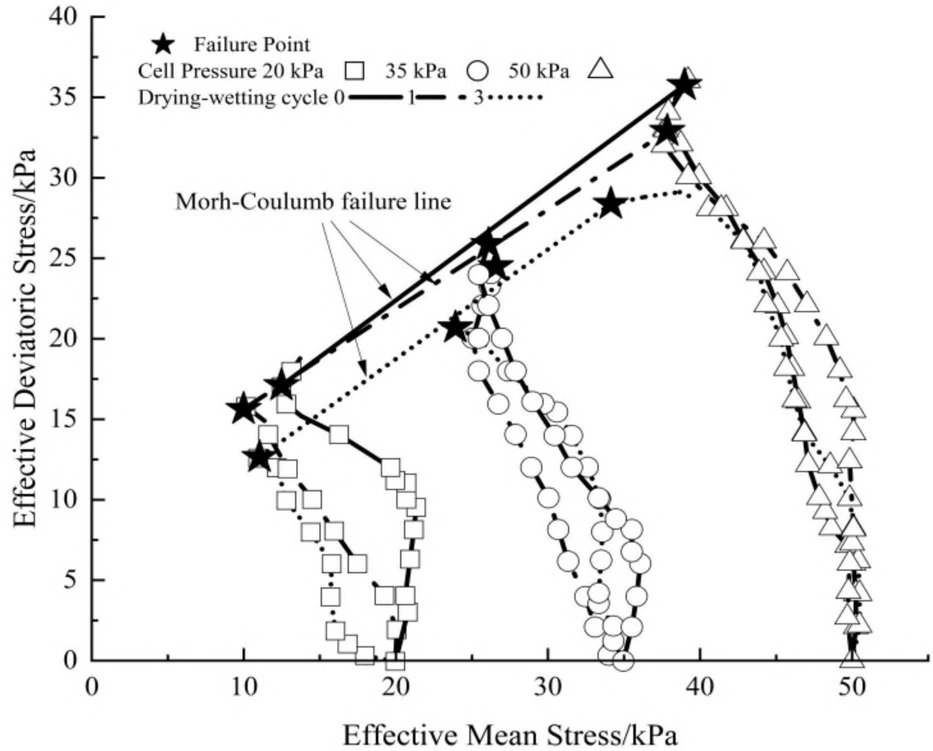

(a) 0 (kPa) Vertical confining pressure

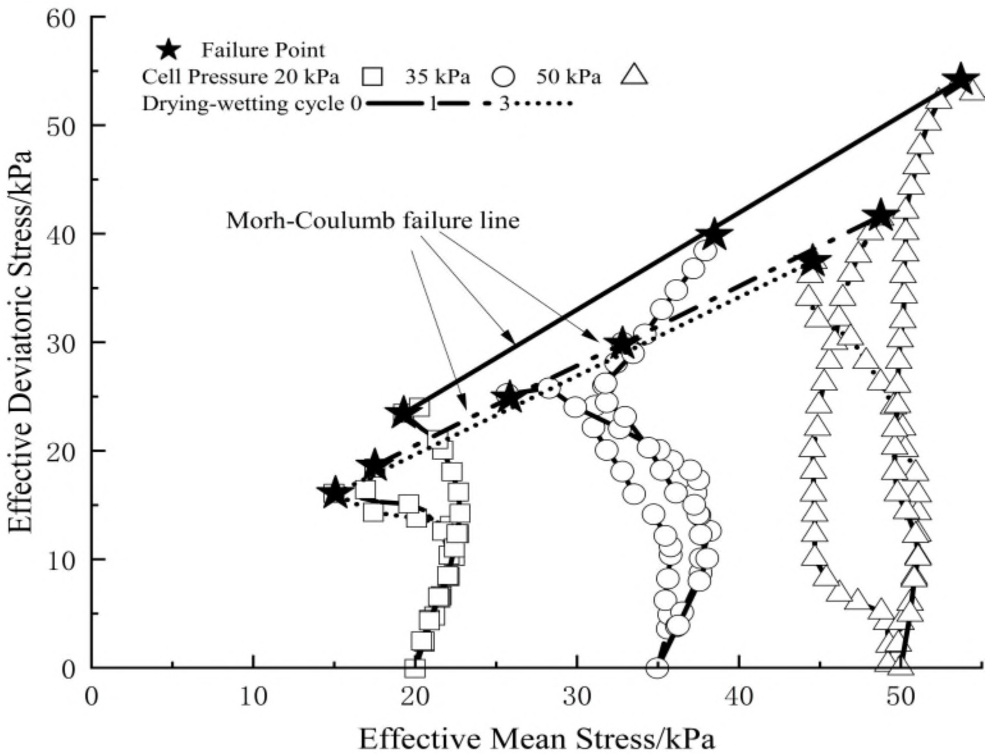

(b) 25 (kPa) Vertical confining pressure

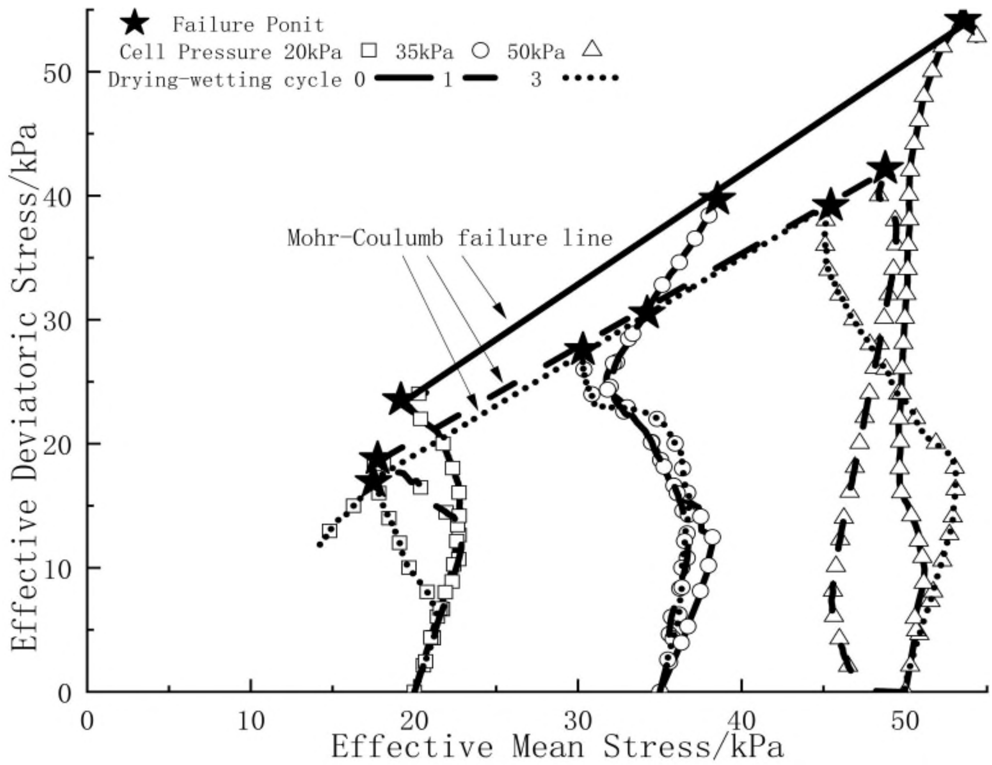

(c)50 (kPa) Vertical confining pressure

Figure 8. The effective stress paths of Mercia Mudstone Clay

Based on Figure 8, in general, the shapes of effective stress paths for original Mercia Mudstone Clay specimens and the specimens subjected to drying-wetting cycles are similar to those of Kaolin Clay specimens, respectively. Additionally, like Kaolin Clay specimens, with the increase of drying-wetting cycle number, the effective deviatoric stress and effective mean stress of failure points for Mercia Mudstone Clay specimens reduce. However, in general, the effective deviatoric stress and effective mean stress of failure points for Mercia Mudstone Clay specimens are larger than those of Kaolin Clay specimens, respectively, and the impacts of drying-wetting cycles on the effective deviatoric stress of failure points for Mercia Mudstone Clay specimens are larger than those of Kaolin Clay specimens. Additionally, as with that of Kaolin Clay, the effective deviatoric stress of failure points for Mercia Mudstone Clay samples under high vertical confining pressure is larger than that under low vertical confining pressure.

5 Conclusion

The main conclusions were summarised as follows:

(1) When subjected to the same number of drying-wetting cycles, the peak shear strength of clayey soil rises with the increase in the vertical confining pressure.

(2) Vertical confining pressure has marginal influence on the pore water pressure of clayey soil subjected to drying-wetting cycles during the triaxial shearing process.

(3) Under the same confining pressure and drying-wetting cycles number, the effective deviatoric stress of failure points for clayey soil under high vertical confining pressure is larger than that under low vertical confining pressure.

(4) The impacts of the first drying-wetting cycle on the hydro-mechanical properties of clayey soil under vertical confining pressures are larger than those during the second and the third cycles, respectively.

(5) Vertical confining pressure can limit the detrimental impacts of drying-wetting cycles on the hydro-mechanical properties of clayey soil effectively. It indicates that imposing vertical confining pressure is an effective method to improve the stability of cover clayey soil in practical engineering facilities when subjecting to drying-wetting cycles.

Acknowledgements

The authors wish to acknowledge the support from China Scholarship Council (CSC) and 2022 Open Project of Failure Mechanics and Engineering Disaster Prevention, Key Lab of Sichuan Province, No FMEDP202209. The paper is also sponsored by Shanghai Sailing Program, No 22YF1415800 and National Natural Science Foundation of China (No. 41772273, No. 42177129).

Conflicts of Interest

The authors declare no conflict of interest.

Data and code Availability Statement

In this paper, all data, models, and code used during the study appear in the submitted article.

References

AC07566974, A. (2003) *Standard test method for measurement of soil potential (suction) using filter paper*. ASTM Internat.

Al-Homoud, A., Basma, A., Husein Malkawi, A. and Al Bashabsheh, M. (1995) 'Cyclic swelling behavior of clays', *Journal of geotechnical engineering*, 121(7), pp. 562-565.

Al-Mahbash, A. M., Elkady, T. Y. & Al-Shamrani, M. A. 2018. Hysteresis soil-water characteristic curves of highly expansive clay. *European Journal of Environmental and Civil Engineering,* 22**,** 1041-1059.

Aldaood, A., Bouasker, M. and Al-Mukhtar, M. (2014) 'Impact of wetting–drying cycles on the microstructure and mechanical properties of lime-stabilized gypseous soils', *Engineering Geology*, 174, pp. 11-21.

ASTM. (2011) *Method for consolidated drained triaxial compression test for soils.*

Bareither, C.A., Edil, T.B., Benson, C.H. and Mickelson, D.M. (2008) 'Geological and physical factors affecting the friction angle of compacted sands', *Journal of geotechnical and geoenvironmental engineering*, 134(10), pp. 1476-1489.

Basma, A.A., Al-Homoud, A.S., Malkawi, A.I.H. and Al-Bashabsheh, M.A. (1996) 'Swelling-shrinkage behavior of natural expansive clays', *Applied Clay Science*, 11(2-4), pp. 211-227.

Chao, Z., Dang, Y., Pan, Y., Wang, F., Wang, M., Zhang, J. and Yang, C. (2023a) 'Prediction of the shale gas permeability: A data mining approach', *Geomechanics for Energy and the Environment*, 2023: 100435.

Chao, Z. and Fowmes, G. (2022) 'The short-term and creep mechanical behaviour of clayey soil-geocomposite drainage layer interfaces subjected to environmental loadings', *Geotextiles and Geomembranes*, 50(2): 238-248.

Chao, Z., Gong, B., Yue, W., Xu, X., Shi, D., Yang, C. and Hu, T. (2022a) 'Experimental study on stress-dependent gas permeability and porosity of artificially cracked cement mortar', *Construction and Building Materials*, 359: 129290.

Chao, Z., Shi, D., Fowmes, G., Xu, X., Yue, W., Cui, P., Hu, T. and Yang, C. (2023b) 'Artificial intelligence algorithms for predicting peak shear strength of clayey soil-geomembrane interfaces and experimental validation', *Geotextiles and Geomembranes*, 51(1): 179-198.

Chao, Z., Wang, M., Sun, Y., Xu, X., Yue, W., Yang, C. and Hu, T. (2022b) 'Predicting stress-dependent gas permeability of cement mortar with different relative moisture contents based on hybrid ensemble artificial intelligence algorithms', *Construction and Building Materials*, 348: 128660.

Cui, C., Liang, Z. Xu, C., Xin, Y. and Wang, B. (2023) 'Analytical solution for horizontal vibration of end-bearing single pile in radially heterogeneous saturated soil', *Applied Mathematical Modelling*, 116:65–83.

Cui, C., Meng, K., Wu Y. and Chapman, D. (2018) 'Dynamic response of pipe pile embedded in layered visco-elastic media with radial inhomogeneity under vertical excitation', *Geomechanics and Engineering*, 16(6):609-618.

Cui, C., Meng, K., Xu, C., Liang, Z., Li, H. and Pei, H. (2021) 'Analytical solution for longitudinal vibration of a floating pile in saturated porous media based on a fictitious saturated soil pile model', *Computers and Geotechnics*, 131:103942.

Cui, C., Meng, K., Xu, C., Wang, B. and Xin Y. (2022) 'Vertical vibration of a floating pile considering the incomplete bonding effect of the pile-soil interface', *Computers and Geotechnics*, 150: 104894.

Cuisinier, O., Stoltz, G. and Masrouri, F. (2014) 'Long-term behavior of lime-treated clayey soil exposed to successive drying and wetting', *Geo-Congress 2014: Geo-Characterization and Modeling for Sustainability*, pp. 4146-4155.

Cui P., Dong Z., Yao X., Cao Y., Sun Y. and Feng L. (2022a) 'What makes urban communities more resilient to COVID-19? A systematic review of current evidence', *International Journal of Environmental Research and Public Health*, 19: 10532.

Cui P., Zou P., Ju X., Liu Y. and Su Y. (2022b) 'Research progress and improvement ideas of anti-epidemic resilience in China's urban communities', *International Journal of Environmental Research and Public Health*, 19 (22): 15293.

Estabragh, A., Parsaei, B. and Javadi, A. (2015) 'Laboratory investigation of the effect of cyclic wetting and drying on the behaviour of an expansive soil', *Soils and foundations*, 55(2), pp. 304-314.

Gastelo, J., Li, D., Tian, K., Tanyu, B.F. and Guler, F.E. (2023) 'Hydraulic conductivity of GCL overlap permeated with saline solutions', *Waste Management*, 157, pp.348-356.

Haghighi, A. (2011) *Thermo-hydro-mechanical behaviour of Kaolin Clay*. Heriot-Watt University.

Hillel, D. (1998) *Environmental soil physics: Fundamentals, applications, and environmental considerations*. Elsevier.

Kong, L., Sayem, H.M. and Tian, H. (2018) 'Influence of drying–wetting cycles on soil-water characteristic curve of undisturbed granite residual soils and microstructure mechanism by nuclear magnetic resonance (NMR) spin-spin relaxation time (T 2) relaxometry', *Canadian Geotechnical Journal*, 55**,** 208-216.

Li, A., Tham, L., Yue, Z., Lee, C. and Law, K. (2005) 'Comparison of field and laboratory soil–water characteristic curves', *Journal of geotechnical and Geoenvironmental Engineering*, 131**,** 1176-1180.

Li, D. and Tian, K. (2022) 'Effects of prehydration on hydraulic conductivity of bentonite-polymer geosynthetic clay liner to coal combustion product leachates', *Geo-Congress*, 568-577.

Li, D., Zainab, B. and Tian, K. (2021) 'Effect of effective stress on hydraulic conductivity of bentonite–polymer geosynthetic clay liners to coal combustion product leachates', *Environmental Geotechnics* 40, 1-12.

Liu, H. (2015) 'Reinforcement load and compression of reinforced soil mass under surcharge loading', *Journal of Geotechnical and Geoenvironmental Engineering*, 141(6), 04015017.

Ma, R., Cai, C., Li, Z., Wang, J., Xiao, T., Peng, G. and Yang, W. (2015) 'Evaluation of soil aggregate microstructure and stability under wetting and drying cycles in two Ultisols using synchrotron-based X-ray micro-computed tomography', *Soil and Tillage Research*, 149, pp. 1-11.

Meng, K., Cui, C., Liang, Z., Li, H. and Pei, H. (2020) 'A new approach for longitudinal vibration of a large-diameter floating pipe pile in visco-elastic soil considering the three-dimensional wave effects', *Computers and Geotechnics*, 128: 103840.

Miao, L., Wang, F., Ye, W., Jiang, M., Li, J. and Shi, S. (2019) 'Combined method limiting shrinkage–swelling behaviours of expansive soils in Huai'an, China', *Environmental Geotechnics*, 8(5), pp. 334-344.

Monroy, R., Zdravkovic, L. and Ridley, A. (2010) 'Evolution of microstructure in compacted London Clay during wetting and loading', *Géotechnique*, 60(2), pp. 105-119.

Nam, S., Gutierrez, M., Diplas, P., Petrie, J., Wayllace, A., Lu, N. and Munoz, J.J. (2010) 'Comparison of testing techniques and models for establishing the SWCC of riverbank soils', *Engineering Geology*, 110**,** 1-10.

Rosone, M., Ferrari, A. and Celauro, C. (2018) 'On the hydro-mechanical behaviour of a lime-treated embankment during wetting and drying cycles', *Geomechanics for Energy and the Environment*, 14, pp. 48-60.

Shao, W., Sun, Q., Xu, X., Yue, W. and Shi, D. (2023) 'Durability life prediction and horizontal bearing characteristics of CFRP composite piles in marine environments', *Construction and Building Materials*, 367: 130116.

Shu, Z., Ning. B., Chen, J., Li, Z., He, M., Luo, J. and Dong H. (2022) 'Reinforced moment-resisting glulam bolted connection with coupled long steel rod with screwheads for modern timber frame structures', *Earthquake Engineering and Structural Dynamics*.

Simms, P.H. and Yanful, E.K. (2001) 'Measurement and estimation of pore shrinkage and pore distribution in a clayey till during soil-water characteristic curve tests', *Canadian Geotechnical Journal*, 38(4), pp. 741-754.

Stoltz, G., Cuisinier, O. and Masrouri, F. (2014) 'Weathering of a lime-treated clayey soil by drying and wetting cycles',. *Engineering Geology*, 181, pp. 281-289.

Tang, C., Wang, D., Shi, B. and Li, J. (2016) 'Effect of wetting–drying cycles on profile mechanical behavior of soils with different initial conditions', *Catena*, 139, pp. 105-116.

Tang, C., Lu, Z. and Yao, H. (2019) 'Effect of axial pressure on lime-treated expansive soil subjected to wetting and drying cycles', *Advances in Civil Engineering*.

Wang, D., Tang, C., Cui, Y., Shi, B., and Li, J. (2016) 'Effects of wetting-drying cycles on soil strength profile of a silty clay in micro-penetrometer tests', *Engineering Geology*, 206, pp. 60-70.

Wang, F., Huang, H., Yin, Z. and Huang, Q. (2022) 'Probabilistic characteristics analysis for the time-dependent deformation of clay soils due to spatial variability', *European Journal of Environmental and Civil Engineering*, 26(12): 6096-6114.

Xu X., Casasayas O., Wang J., Mao P. and Cui P. (2022) 'Stakeholder-associated impact factors of building energy performance gap and their intersections: A social network analysis', *Journal of Cleaner Production*, 370: 133228.

Zainab, B., Wireko, C., Dong, L., Tian, K., Tarek., K. (2021) 'Hydraulic conductivity of bentonite-polymer geosynthetic clay liners to coal combustion product leachates', G*eotextiles and Geomembranes*, 49 (5), 1129-1138.

Zeng, L., Cui, Y., Conil, N., Zghondi, J., Armand, G. and Talandier, J. (2017) 'Experimental study on swelling behaviour and microstructure changes of natural stiff Teguline clays upon wetting', *Canadian Geotechnical Journal*, 54(5), pp. 700-709.

Zhang, J., Jiang, T., Wang, X., Liu, C. and Huang, Z. (2018) 'Influences of drying and wetting cycles and compaction degree on strength of Yudong silt for subgrade and its prediction', *Advances in Civil Engineering 2018*.

Zhang, W., Shi, D., Shen, Z., Shao, W., Gan, L., Yuan, Y., Tang, P., Zhao, S. and Chen, Y. (2023a) 'Reduction of the calcium leaching effect on the physical and mechanical properties of concrete by adding chopped basalt fibers', *Construction and Building Materials*, 365: 130080.

Zhang, W., Shi, D., Shen, Z., Wang, X., Gan, L., Shao, W., Tang, P., Zhang, H. and Yu, S. (2023b) 'Effect of calcium leaching on the fracture properties of concrete', *Construction and Building Materials*, 365: 130018.